

Tunable aggregation-induced emission of diphenyldibenzofulvenes†

Hui Tong,^a Yongqiang Dong,^{ab} Matthias Häußler,^a Jacky W. Y. Lam,^a Herman H.-Y. Sung,^a Ian D. Williams,^a Jingzhi Sun^b and Ben Zhong Tang^{*ab}

Received (in Cambridge, UK) 9th November 2005, Accepted 11th January 2006

First published as an Advance Article on the web 25th January 2006

DOI: 10.1039/b515798f

Nonemissive fulvenes can be induced to luminesce by aggregate formation, with the crystalline aggregates emitting bluer lights more intensely than their amorphous counterparts.

When chromophoric molecules are dispersed in aqueous media or fabricated into solid films, they tend to aggregate, due to the strong electronic and hydrophobic interactions between their aromatic rings in the polar environment or in the solid state. The aggregate formation often quenches light emission, which has been a thorny problem in the development of efficient environmental sensors, biological probes, and light-emitting diodes.^{1–3} We have recently observed an unusual phenomenon of aggregation-induced emission (AIE): a group of nonemissive silole molecules have been induced to emit intensely by aggregate formation.^{4,5} While crystallization commonly weakens and red-shifts light emission, the crystalline aggregates of the siloles are found to emit stronger, bluer lights than their amorphous counterparts.⁶ The AIE phenomenon poses a challenge to our current understanding of light-emitting processes in the solid state, which may spawn new photophysical theories and spur technological innovations. Because of its obvious academic value and practical implication, we have worked on the exploration of more AIE systems.⁷ In this paper, we report our results on the development of a new class of AIE molecules based on a fulvene scaffold structure. Different from the organometallic silole species, the fulvenes are pure organic dyes containing no metalloids atoms.

The fulvene derivatives were prepared by the synthetic routes shown in Scheme S1 (ESI). The lithiation of fluorene followed by the reaction of the intermediate with 2-aminobenzophenone gave a diphenyldibenzofulvene derivative with an amino substituent (**1**). The treatments of **1** by acetic acid and trifluoroacetic acid yielded the acylation products carrying acetyl (**2**) and trifluoroacetyl groups (**3**), respectively. All the fulvene derivatives were characterized by standard spectroscopic methods, from which satisfactory analysis data corresponding to their expected molecular structures were obtained (see ESI for details). The fulvene dyes are all soluble

in common organic solvents such as acetonitrile, chloroform and THF but are insoluble in water.

Dilute acetonitrile solutions of all the three fulvene derivatives are practically nonluminescent. However, addition of water, a non-solvent of the fulvenes, can greatly affect their photoluminescence (PL) processes (Figs. S1–S3 in the ESI). The isolated species of **1** in the molecularly dissolved solution displays a PL spectrum that is almost a flat line parallel to the abscissa (Fig. 1A). Upon addition of a large amount of water, the mixture becomes visually emissive (see, for example, the photo shown in the graphical abstract). The emission and absorption spectra of **1** both red-shift with the addition of water (Table 1), suggestive of the formation of J-aggregates in the aqueous mixture.⁸ Clearly, the emission of **1** is induced by the aggregate formation, or in other words, **1** is AIE-active. Whereas many dye suspensions in aqueous media gradually bleach or fade with time, the AIE system of **1** is very stable: little, if any, change is detected in the PL spectra of its nanoaggregates in the aqueous mixtures even after the suspensions have been stored under ambient conditions without protection from light and air for more than two months.

Careful analysis of the PL spectra of **1** in the aqueous mixtures reveals a decrease in its emission intensity and a red-shift in its emission maximum (λ_{em}) when the water content is changed from 95 to 99 vol% (Fig. S1 in the ESI). We speculate that this is due to the change in the packing order of the aggregates from a crystalline state to an amorphous one. In a mixture with a “lower” water ratio ($\leq 95\%$), the molecules of **1** may slowly assemble in an ordered fashion to form more emissive, “bluer”, crystalline clusters, while in a mixture with a “higher” water ratio (99%), the molecules of **1** may quickly agglomerate in a random way to form less emissive,

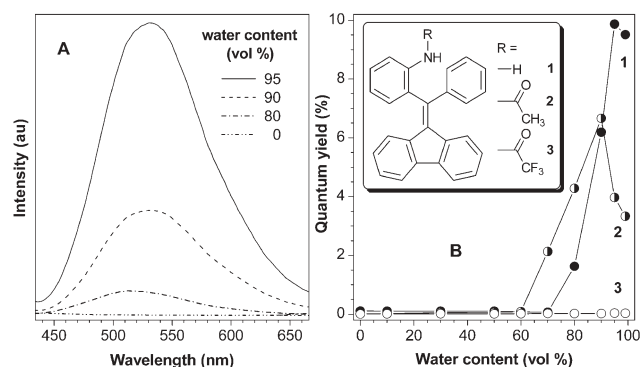


Fig. 1 (A) Emission spectra of **1** in acetonitrile/water mixtures and (B) dependence of quantum yields of fulvenes **1–3** on solvent compositions of the acetonitrile/water mixtures. Fulvene concentration: 10 μ M; excitation wavelength: 350 nm.

^aDepartment of Chemistry, The Hong Kong University of Science & Technology, Clear Water Bay, Kowloon, Hong Kong, China.

E-mail: tangbenz@ust.hk; Fax: +852-2358-1594; Tel: +852-2358-7375

^bKey Laboratory of Macromolecular Synthesis and Functionalization of the Ministry of Education, Department of Polymer Science and Engineering, Zhejiang University, Hangzhou 310027, China

† Electronic supplementary information (ESI) available: Preparation and characterization details for fulvenes **1–3**, absorption and emission spectra of **1–3** in solution and aggregation states, emission spectra of **1** and **2** in amorphous and crystalline states, optimized geometric structures and molecular orbital amplitude plots of HOMOs and LUMOs of **1–3**, and single crystal data of **1**. See DOI: 10.1039/b515798f

Table 1 Absorption and emission properties of diphenyldibenzofulvenes in solution (Soln),^a aggregate (Aggr),^b crystalline (Cryst), and amorphous (Amor) states

	λ_{ab} , nm ^c		λ_{em} , nm ^d		Cryst	Amor
	Soln	Aggr	Soln (Φ_F)	Aggr (Φ_F)		
1	316	335	439 (0.11)	545 (9.50)	527	550
2	326	338	437 (0.02)	483 (3.30)	465	487
3	337	353	440 (0.01)	465 (0.03)		

^a In acetonitrile solutions (10 μ M). ^b In acetonitrile/water (1:99 by vol) mixtures (10 μ M). ^c Absorption maximum. ^d Emission maximum [with quantum yield (Φ_F , %) given in the parentheses]; excitation wavelength: 350 nm.

“redder”, amorphous powders. This is proved to be the case by the electron microscopy and diffraction analyses, which confirm that the nanoparticles formed in the mixtures with “lower” and “higher” water contents are indeed crystalline and amorphous, respectively (Fig. S5 in the ESI).

The dependence of the fluorescence quantum yield (Φ_F) of **1** on the solvent composition of the acetonitrile/water mixture is shown in Fig. 1B. In the mixtures with water contents below $\sim 70\%$, the Φ_F values of **1** are very small because its molecules are dissolved in the mixtures. Its Φ_F starts to increase at a water content of $\sim 70\%$, suggesting that its molecules begin to aggregate in the mixture with this solvent composition. The Φ_F of **1** continuously increases with an increase in the water content, reaching a maximum of 9.8% at a water content of 95%, which is ~ 90 -fold higher than that of its dilute acetonitrile solution. Further increasing the water content to 99% results in a decrease in Φ_F (9.5%) due to the morphological change discussed above. It should be pointed out that the absolute Φ_F values of the aggregates of **1** could be much higher than its relative values given in Fig. 1B and Table 1, as the apparent high absorbance caused by the light-scattering or Mie effect of the nanoparticle suspensions⁹ results in underestimations of the relative Φ_F values.^{4,10}

Similar to **1**, its derivative carrying an acetyl group (**2**) also shows typical AIE behaviours (Fig. S2 in the ESI). Whereas its acetonitrile solution is virtually nonluminescent with a near-zero PL efficiency ($\Phi_F = 0.016\%$), its aggregates are emissive. Its Φ_F displays a similar trend to that of **1** (Fig. 1B). At a water content of 90%, its Φ_F is increased to 6.6%, which is two orders of magnitude (or 416-fold) higher than that of its acetonitrile solution. Again, at very high water contents, its Φ_F drops. Close inspection reveals that the λ_{em} 's of the aggregates of **2** are blue-shifted from those of **1**. The steric hindrance of acetylamino group of **2** may have weakened the intermolecular electronic interaction and the hydrogen bonding between the amide groups may have changed the packing structure: both of these two effects may have contributed to the blue-shift in the λ_{em} 's of its aggregates.

In sharp contrast to **1** and **2**, their congener bearing a trifluoroacetylamino group (**3**) is totally AIE inactive. Its dilute solution is nonemissive ($\Phi_F = 0.009\%$), and adding water exerts little effect on its emission efficiency. The photoinduced electron-transfer caused by the strong electron-withdrawing trifluoroacetyl group may have effectively quenched its PL in the solution and solid states. It now becomes clear that the AIE process of fulvene can be turned on and off by a simple structural modification of its substituent.

After studying the optical properties of the fulvenes in the liquid media (acetonitrile solvent and aqueous mixtures), we investigated their PL behaviours in the solid state. We prepared two kinds of solid samples: a crystalline chunk and an amorphous powder. The crystals of **1** and **2** emit bluer lights more efficiently, in comparison to their amorphous cousins (Fig. S4 in the ESI). This agrees well with our finding described above: the crystalline aggregates of **1** and **2** in the aqueous mixtures emit stronger, bluer lights than their amorphous ones (Figs. 1B and S5). However, different from other AIE molecules,^{4,11} **1** and **2** remain nonemissive after they are doped into poly(methyl methacrylate) (PMMA) films ($\Phi_F \leq 0.5\%$). This suggests that the molecular interactions play an important role in the AIE processes of the fulvenes. The PMMA matrix serves as a solid “solvent”, which separates the fulvene molecules and impedes their aggregate formation. As expected, almost no PL signals can be captured from **3** in all the cases.

In an effort to understand the photophysical processes of **1–3**, we calculated their geometric structures at the RHF/6-31G* level (Fig. S6 in the ESI).¹² On the basis of the optimized geometries, their electronic spectra were computed by the semi-empirical ZINDO/S method in the HyperChem.¹³ The calculated absorption maximum ($\lambda_{ab,c}$) of **1** is 317 nm, agreeing well with its experimental value ($\lambda_{ab} = 316$ nm). Although $\lambda_{ab,c}$'s of **2** (318 nm) and **3** (322 nm) slightly differ from their λ_{ab} 's, the trend towards a bathochromic shift is consistent with the experimental result. The HOMOs and LUMOs of **1–3** are all dominated by the orbitals originating from their diphenyldibenzofulvene core, with extremely low electron densities at the amino and amide pendants (Figs. S7–S9 in the ESI). This explains why the emissions from all the three fulvene derivatives in the acetonitrile solutions are almost the same, independent of their substituent groups.¹⁴

To identify the origin of the AIE phenomenon of the fulvenes, their molecular geometries and electronic structures in the solid state need to be investigated. Delightfully, the crystal structure of **1** can be determined by the X-ray diffraction (XRD) measurement.† As can be seen from Fig. 2A, there exist two fulvene molecules in one asymmetric unit that mainly differ in the torsion angles of the phenyl groups with respect to the dibenzofulvene ring, presumably as a result of the C–H \cdots π and N–H \cdots π intermolecular interactions (Fig. 2B).^{3c}

On the basis of these geometric structures, the electronic spectra of **1** in different packing states are computed using the ZINDO/S method.¹⁵ For a single molecule of **1**, three possible nonradiative transitions (with zero oscillator strength) at 437, 524 and 539 nm are found, which may have served as the nonradiative decay paths that effectively quenched the PL of **1** in the dilute solution. In the crystalline state (Fig. 2B), a set of three other possible nonradiative transitions at 439, 442 and 447 nm are identified, which obviously cannot quench the strong emission of the crystal of **1** at 527 nm. From the solution state to the crystalline state, the nonradiative transition of **1** at ~ 527 nm disappears. Clearly the closure of this nonradiative channel has endowed **1** with the AIE property. This channel closure is perhaps caused by the restriction of molecular motions due to the strong intermolecular interactions in the fulvene aggregates. On the other hand, the nonradiative transition at ~ 439 nm always exists, which makes this emission invisible even in the solid state.

The structure shown in Fig. 2A may serve as a model for the amorphous state, where the intermolecular interactions are limited

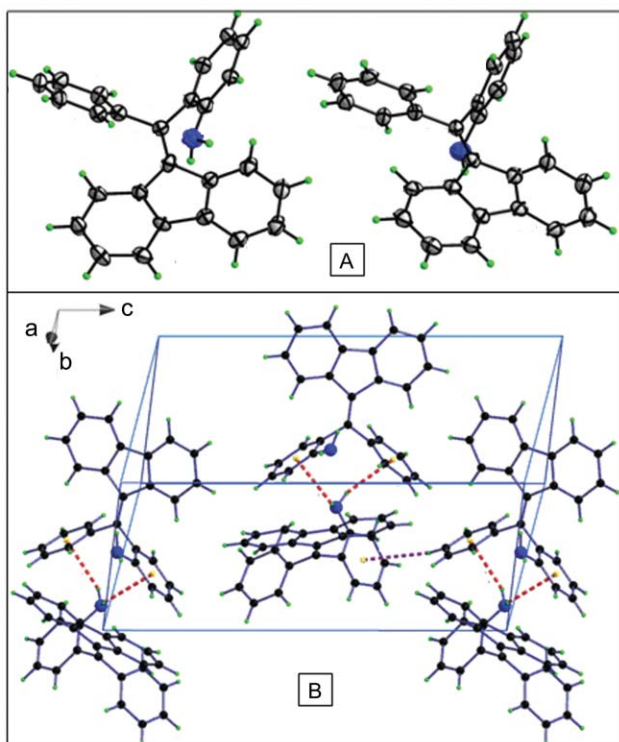


Fig. 2 (A) Molecular structures of two molecules of **1** in an asymmetric unit and (B) perspective view of crystal packing of molecules of **1**, some of whose N–H... π and C–H... π hydrogen bonds are shown by the dotted lines (see Fig. S11 in the ESI for a more completed picture).

to a short range. The computation for **1** in this packing state reveals four possible nonradiative transitions at 434, 447, 521 and 522 nm. The later two relaxation pathways are close to the λ_{em} of its crystal (527 nm), suggesting that the weaker emission at 550 nm in the amorphous state is the result of a partially quenched emission.

Thanks to the geometric structures obtained from its XRD data, the AIE phenomenon of **1** can be readily explained. Unfortunately, however, similar calculation cannot be performed on **2**, because its single crystal structure is unavailable. The ZINDO/S calculation based on its optimized single molecular structure, however, reveals two possible nonradiative transitions at 435 and 472 nm, which are very close to its λ_{em} . These nonradiative decay channels effectively quench its PL in the dilute solution, thus making its isolated species nonemissive.

In summary, we have investigated the photophysical processes of three novel fulvene derivatives. We have proved that **1** and **2** are AIE-active and demonstrated that the fulvene emission can be tuned by changing the substituent structure and by varying the aggregate morphology. We have further shown that the blockage of the nonradiative channel of **1** at ~ 527 nm is the cause of its AIE behaviours. The fulvene-based AIE molecules may find an array of high-tech applications as luminescent and sensory materials in optical display, environmental protection, and biomedical imaging.

This project was partially supported by the Hong Kong Research Grants Council, the National Science Foundation and the Ministry of Science and Technology of China. We are grateful

to the group of Prof. Y. Luo at the Royal Institute of Technology in Sweden for its technical assistance in the theoretical calculations. B.Z.T. thanks the support from the Cao Guangbiao Foundation of the Zhejiang University.

Notes and references

† Crystal data for **1**: $\text{C}_{26}\text{H}_{19}\text{N}$, $M = 345.42$, monoclinic, $P2(1)$, $a = 10.6320(18)$, $b = 9.2506(15)$, $c = 18.993(3)$ Å, $\beta = 105.409(3)^\circ$, $V = 1800.8(5)$ Å³, $Z = 4$, $D_c = 1.274$ Mg m⁻³, $\mu = 0.073$ mm⁻¹, $F(000) = 728$, $T = 100(2)$ K, $2\theta_{\text{max}} = 25.00^\circ$, 10729 measured reflections, 4273 independent reflections ($R_{\text{int}} = 0.0543$), $R_1 = 0.0768$, $wR_2 = 0.1450$ (all data), $\Delta\rho = 0.334$ and -0.219 e Å⁻³. CCDC 289588. For crystallographic data in CIF or other electronic format see DOI: 10.1039/b515798f

- (a) S. J. Toal, K. A. Jones, D. Magde and W. C. Troglor, *J. Am. Chem. Soc.*, 2005, **127**, 11661; (b) C. J. Bhongale, C.-W. Chang, C.-S. Lee, E. W.-G. Diau and C.-S. Hsu, *J. Phys. Chem. B*, 2005, **109**, 13472; (c) Z. Xie, B. Yang, F. Li, G. Cheng, L. Liu, G. Yang, H. Xu, L. Ye, M. Hanif, S. Liu, D. Ma and Y. Ma, *J. Am. Chem. Soc.*, 2005, **127**, 14152; (d) J. Ohshita, K. Lee, M. Hashimoto, Y. Kunugi, Y. Harima, K. Yamashita and A. Kunai, *Org. Lett.*, 2002, **4**, 1891; (e) B. K. An, S. K. Kwon, S. D. Jung and S. Y. Park, *J. Am. Chem. Soc.*, 2002, **124**, 14410.
- (a) C. P.-Y. Chan, M. Häußler, B. Z. Tang, Y. Q. Dong, K. Sin, W.-C. Mak, D. Trau, M. Seydack and R. Renneberg, *J. Immunolog. Methods*, 2004, **295**, 111; (b) J. W. Y. Lam and B. Z. Tang, *Acc. Chem. Res.*, 2005, **38**, 745.
- (a) C. W. Tang and S. A. Van Slyke, *Appl. Phys. Lett.*, 1987, **51**, 913; (b) A. Kraft, A. C. Grimsdale and A. B. Holmes, *Angew. Chem. Int. Ed.*, 1998, **37**, 402.
- (a) J. Luo, Z. Xie, J. W. Y. Lam, L. Cheng, H. Chen, C. Qiu, H. S. Kwok, X. Zhan, Y. Liu, D. Zhu and B. Z. Tang, *Chem. Commun.*, 2001, 1740; (b) J. Chen, C. W. Law, J. W. Y. Lam, Y. Dong, S. M. F. Lo, I. D. Williams, D. Zhu and B. Z. Tang, *Chem. Mater.*, 2003, **15**, 1535; (c) G. Yu, S. Yin, Y. Liu, J. Chen, X. Xu, X. Sun, D. Ma, X. Zhan, Q. Peng, Z. Shuai, B. Z. Tang, D. Zhu, W. Fang and Y. Luo, *J. Am. Chem. Soc.*, 2005, **127**, 6335; (d) B. Mi, Y. Dong, Z. Li, J. W. Y. Lam, M. Haussler, H. Y. Sung, H. S. Kwok, Y. Dong, I. D. Williams, Y. Liu, Y. Luo, Z. Shuai, D. B. Zhu and B. Z. Tang, *Chem. Commun.*, 2005, 3583; (e) Y. Dong, J. W. Y. Lam, Z. Li, H. Tong, Y. Dong, X. Feng and B. Z. Tang, *J. Inorg. Organomet. Polym. Mater.*, 2005, **15**, 287.
- M. Freemantle, *Chem. Eng. News*, 2001, **79**(41), 29.
- (a) Z. Li, Y. Dong, B. Mi, Y. H. Tang, M. Häußler, H. Tong, Y. Dong, J. W. Y. Lam, Y. Ren, H. Y. Sung, K. S. Wong, P. Gao, I. D. Williams, H. S. Kwok and B. Z. Tang, *J. Phys. Chem. B*, 2005, **109**, 10061; (b) J. Chen, B. Xu, K. Yang, Y. Cao, H. Y. Sung, I. D. Williams and B. Z. Tang, *J. Phys. Chem. B*, 2005, **109**, 17086.
- (a) H. Tong, Y. Dong, M. Häußler, Z. Li, B. Mi, H. S. Kwok and B. Z. Tang, *Mol. Cryst. Liq. Cryst.*, 2006, **446**, 183; (b) J. Chen, B. Xu, X. Ouyang, B. Z. Tang and Y. Cao, *J. Phys. Chem. A*, 2004, **108**, 7522.
- L. D. Lu, R. Helgeson, R. M. Jones, D. McBranch and D. Whitten, *J. Am. Chem. Soc.*, 2002, **124**, 483.
- B. Z. Tang, Y. Geng, J. W. Y. Lam, B. Li, X. Jing, X. Wang, F. Wang, A. Pakhomov and X. X. Zhang, *Chem. Mater.*, 1999, **11**, 1581.
- All the absolute quantum yields ($\Phi_{\text{F,a}}$) of the AIE-active siloles are higher than their relative ones ($\Phi_{\text{F,r}}$): for example, $\Phi_{\text{F,a}}$ of 1-methylpentaphenylsilole (85%)^{4c} is 4-fold higher than its $\Phi_{\text{F,r}}$ (21%)^{4a}.
- (a) S. Jayanty and T. P. Radhakrishnan, *Chem. Eur. J.*, 2004, **10**, 791; (b) H. J. Tracy, J. L. Mullin, W. T. Klooster, J. A. Martin, J. Haug, S. Wallace, I. Rudloe and K. Watts, *Inorg. Chem.*, 2005, **44**, 2003.
- Gaussian 98 (Revision A.7)*, Gaussian, Inc., Pittsburgh, PA, 1998.
- Hyperchem Release 7. Windows Molecular Modeling System, Hypercube, Inc. and Autodesk, Inc. Developed by Hypercube, Inc.
- C. Risko, G. P. Kushto, Z. H. Kafati and J. L. Bredas, *J. Chem. Phys.*, 2004, **121**, 9031.
- (a) N. DiCesare, M. Belletete, M. Leclerc and G. Durocher, *J. Phys. Chem. A*, 1999, **103**, 803; (b) N. DiCesare, M. Belletete, E. R. Garcia, M. Leclerc and G. Durocher, *J. Phys. Chem. A*, 1999, **103**, 3864.